Modulation bandwidth studies of recombination processes in blue and green InGaN quantum well micro-light-emitting diodes

Richard P. Green,[1, a)] Jonathan J. D. McKendry,[2] David Massoubre,[2] Erdan Gu,[2] Martin D. Dawson,[2] and A. E. Kelly[3]

[1)] *Dept. of Physics, University College Cork, Cork, Ireland*

[2)] *Institute of Photonics, SUPA, University of Strathclyde, Glasgow, G4 0NW, UK*

[3)] *School of Engineering, University of Glasgow, Glasgow, G12 8QQ, UK*

We report modulation bandwidth measurements on a number of InGaN-based quantum well LEDs emitting at 450 and 520nm wavelengths. It is shown that for these devices the data can be interpreted in terms of Auger recombination, by taking account of the carrier density dependence of the radiative coefficient. We find values for the Auger coefficient of $(1\pm0.3)\times10^{-29}\mathrm{cm}^6\mathrm{s}^{-1}$ at 450nm and $(3\pm1)\times10^{-30}\mathrm{cm}^6\mathrm{s}^{-1}$ at 520nm.

PACS numbers: 78.60.Fi Electroluminescence, 78.66.Fd Optical properties of III-V semiconductors, 42.72.Bj Visible and UV sources.

There is much current interest in the recombination processes governing carrier lifetimes in GaN-based LED structures. One reason for this is that the maximum modulation speeds attainable with these devices are governed by the carrier lifetimes within the quantum wells (QWs). Recent reports have raised the possibility of using GaN based visible-emitting LEDs for data transfer either in free space or plastic optical fibre.[1–3] These have included demonstration[2] of error-free data transmission at rates up to 1Gbit/s. Fast modulation speeds would also be advantageous for the use of these devices in time-resolved fluorescence measurements.[4]

There is also great interest because of the importance of these processes in the effect known as 'droop', where–except at very low current densities below a few tens of A cm^{-2}–the quantum efficiency of GaN LEDs decreases with applied current.[5] There is much controversy over the physical mechanisms causing droop. Suggested candidates for this include Auger recombination,[6,7] carrier overflow[8,9] and unusual defect behavior.[10,11] To engineer devices with high efficiencies or those capable of being modulated at high rates, a thorough understanding of the physics governing the carrier density dependence of non-radiative processes in GaN LEDs is needed.

The objective of the present work is to investigate whether differential lifetimes in GaN-based micro-LEDs (μLEDs) can be described by the simple ABC model that is successful in describing carrier lifetimes in narrow-gap semiconductors.[12] This rate equation model considers that the current through the device is made up of three contributions; a non-radiative current due to Shockley-Read-Hall (SRH) recombination at defect sites, a current due to radiative recombination of electrons and holes, and an Auger current. The total current is thus:

$$I = I_A + I_B + I_C = ead\left(AN + BN^2 + CN^3\right) \qquad (1)$$

[a)] Electronic mail: r.green@ucc.ie

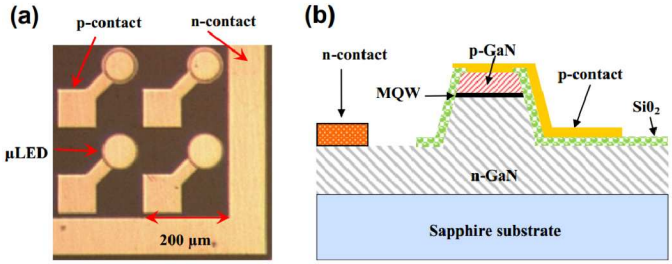

FIG. 1. (a): Plan view micrograph, showing four four representative $\mu-$LEDs. (b): Schematic cross-section of the device structure used.

where N is the carrier density (per unit volume) within the QWs and A, B and C the SRH, radiative and Auger coefficients respectively. The electronic charge is denoted by e while a and d are the device area and the total thickness of the QWs respectively. The differential lifetime τ is then given by the derivative of the recombination rate with respect to carrier density:[12]

$$\tau^{-1} = A + 2BN + 3CN^2 \qquad (2)$$

This simple model is made under the assumption that A, B and C are independent of N, and the carrier density is the same in all QWs. In fact, when working with narrow-gap materials such as InGaAs, good agreement with experiment can only be found over a large range of carrier densities if B is a decreasing function of N. This is attributed to a reduction in the optical matrix element for the interband transitions as carriers begin to fill states away from the Γ point.[13] This can be described by the empirical formula[14]

$$B(N) = \frac{B_0}{1 + N/N_0} \qquad (3)$$

or by a linear approximation to this.

We carried out measurements of the differential lifetime in InGaN based μLEDs as a function of bias current, in order to test the applicability of the above model. The

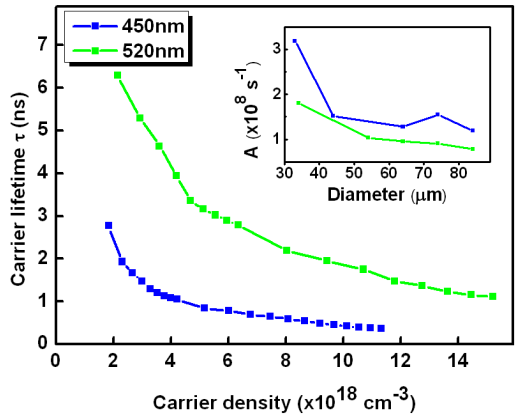

FIG. 2. (Main part): Carrier lifetimes obtained through Eq. 4 as a function of the QW carrier density for two representative devices; a 44μm diameter LED emitting at 450nm, and a 54μm diameter 520nm emitter. (Inset): The A-coefficients deduced from the measured data from micro-LEDs of differing sizes for the two wavelengths.

μLEDs were fabricated from standard commercial MQW wafers, emitting at 450nm or 520nm into 24-84μm diameter mesas. The combined thickness of the quantum wells within each wafer was 14nm. A plan view and schematic cross-section of the device structure are shown in Fig. 1 (a) and (b) respectively. Full details of device design and fabrication techniques have been given elsewhere.[1,2]

Each LED was contacted using a high speed (40GHz bandwidth) ground-signal-ground probe, and the frequency response was measured under a range of biases using a network analyser and a high-speed silicon photodetector (Newport 818-BB21A). The differential carrier lifetime is related to the -3dB point of the frequency response[15] as

$$\tau^{-1} = 2\pi f_{3dB}. \quad (4)$$

By using μLEDs, we were able to ensure that the device bandwidth was determined by the carrier lifetime, rather than the device capacitance. We confirmed this by comparing results obtained from devices of different diameter; the value of τ at a given current density was very similar for all devices measured (see Fig. 5 in Ref. 2). The material properties obtained in this way would also be applicable to larger devices made from the same wafer.

From this data, it is possible to obtain the QW carrier densities corresponding to a given current I through the integral:[16]

$$N(I) = \frac{\eta_{inj}}{ead}\int_0^I \tau \mathrm{d}I \quad (5)$$

η_{inj} represents the injection efficiency of the carriers into the QWs. For the present we assume this to be independent of the injection current; this will be discussed later. A value of 0.7 is used as reported by Scheibenzuber *et al*,[7] based on slope efficiency measurements of GaN-based laser diodes. We find that the values of B and C obtained exhibit relatively small changes when this parameter is varied. A change from $\eta_{inj} = 0.7$ to 0.6 results in a 30% increase in the value obtained for B, much smaller than that due to the uncertainty in the value of injection efficiency, as discussed below. The same change in η_{inj} results in a ∼60% increase in the value of C obtained. The significance of this will be discussed below.

To give a more robust fitting of the lifetime data to the ABC model, we used an independent means of establishing values for B, based on the relationship between spontaneous emission power and current (the LI curve). The output power was measured using a calibrated 12mm diameter Si photodetector placed in close proximity above the device. This LI measurement gives a reliable determination of the shape of the $B(N)$ versus N curve. This will also give accurate values for B, if it is combined with a knowledge of the proportion of photon emitted by the MQWs which are incident on the photodiode (the collection efficiency, η_{coll}). It is difficult to estimate the value of η_{coll}, due to the substrate emitting geometry of our devices, and the fact that scattering of light from the mesa sidewalls will play a much more significant rôle in μLEDs than in larger devices. Nevertheless, there are certain clear statements that we can make about η_{coll} for the devices used in this work. Firstly, the 450nm emitting devices were grown on a patterned sapphire substrate designed to enhance the proportion of light escaping. Huh *et al*[17] reported that this resulted in an increase in emitted light of ∼ 33% (for top surface collection) and ∼ 19% (for substrate side collection. The μLEDs reported here are in flip-chip format with a reflective p-contact, so we consider that η_{coll} for the 450nm devices is likely to be about 50% higher than would be the case for an equivalent structure grown on a plain substrate, and will be higher than that for the 520nm devices.

We can estimate a lower bound for η_{coll} using a simple model of the Fresnel reflectivity at the GaN-sapphire and sapphire-air interfaces. Because this does not include the effects of either multiple reflections or scattering from mesa sidewalls, this will provide an underestimate for η_{coll}. This model suggests that a suitable lower bound will be η_{coll}(min)=4% (520nm) and 6.6% (450nm, including the substrate effect). The work by Lee *et al*[18] provides a corresponding upper bound. They analysed the light emission from a variety of LED geometries using a Monte-Carlo ray tracing technique. Based on this, we expect that η_{coll}(max)= 30% (450nm) and 20% (520nm). The data presented in this paper uses midpoint values of η_{coll}=18% (450nm) and 12% (520nm). While this uncertainty will have a strong effect on the values we obtain for B, its effect on C is small, as will be discussed later.

The carrier density dependence of B obtained from these measurements is shown in Fig. 3. A number of significant features are visible in this. The values of B found for the 520nm emitting devices are generally

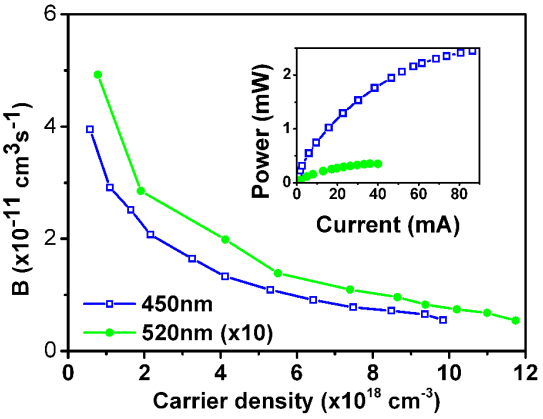

FIG. 3. (Main part): Values of the radiative coefficient B obtained from the LI curves for 44μm diameter 450nm emitting and 54μm diameter, 520nm emitting devices. These are plotted against the carrier densities N obtained through Eq. 5. Note that the 520 nm data is plotted on an expanded vertical scale. (Inset): LI data for the same two devices.

an order of magnitude below those of the 450nm devices. The lower B coefficient found for our 520nm emitting device is consistent with literature reports showing that the internal quantum efficiency of green-emitting InGaN LEDs is lower than their blue-emitting counterparts. This phenomenon is commonly referred to as the 'green gap' or 'green-yellow gap' and may be attributed to stronger piezoelectric and spontaneous polarisation effects in higher indium content InGaN devices.[19] Laubsch *et al*[20] reported values of B in the region of 1.2×10^{-12}cm^{3}s^{-1} for a 520nm emitting device, compatible with those shown in Fig. 3. In contrast, the values of B reported for blue-emitting devices are larger; Meneghini *et al*[21] report $B \sim 1 - 2 \times 10^{-11}$cm^{3}s^{-1} for 450nm emitting LEDs, which are close to the values we obtain at high currents. The decrease in the observed value of B with carrier density is generally attributed to the effects of phase space filling.[13] We observe a reduction in B of about 80% over the current range measured. This large change is attributed to the high current densities attainable in the μLED geometry used in this work.

The task of finding values for A and C is now simplified by having an independent means of studying the carrier density dependence of B. From inspection of Eq. 2, it is apparent that A can be found by extrapolating the data in Fig. 2 back to the $N = 0$ axis. The values of A obtained were in the range $1.2 - 3.2 \times 10^8$s^{-1} for the 450nm devices, and $0.8 - 1.8 \times 10^8$s^{-1} for the 520nm ones. These are within the range of those which have previously been published.[14,22] One possible reason for the consistently lower values of A found for the 450nm emitting devices is the use of a patterned substrate; this has previously been associated with a lower dislocation density.[23] For both wavelengths, a clear dependence of A on the device diameter was observed, as seen in the inset to Fig. 2. This is attributed to the greater influence of surface effects on the smaller devices, with a high density of recombination sites at the edge of the mesa arising from ICP etching during the fabrication process. A similar dependence of A on the device diameter has been reported for GaAs/AlGaAs VCSEL devices of similar size.[24]

The above discussion gives a method of estimating the portion of the total current through the device due to recombination at defect sites, and that due to radiative recombination. We assume here that all the remainder of the current is due to Auger recombination, and we denote this I_C, as defined in Eq. 1. This implies that the value of C will be given by:

$$C = \frac{1}{ead}\frac{\partial I_C}{\partial (N^3)} \tag{6}$$

Fig. 4 (a) shows the values of I_C obtained for two representative devices, plotted against N^3. Except at very low carrier densities, the data can be fitted to a straight line, indicating that the Auger coefficient is not significantly changing over this range. This fitting process was carried out for a number of devices of different diameters and the two wavelengths being considered. The values of C obtained from this process were $C_{450} = (1\pm0.3)\times10^{-29}$cm^{6}s^{-1} and $C_{520} = (3\pm1)\times10^{-30}$cm^{6}s^{-1}. There was no trend observed in the value found for C for devices of different diameters. These values are shown in Fig. 4 (b), together with a number of experimental and theoretical values for C which have previously been reported in the literature.

We now consider the influence that the uncertainty in our estimate of the collection efficiency has on the results we have obtained. Since the values of A are obtained directly from the differential lifetime measurements, this will be unaffected by any such error. It is similarly obvious that the values of B (at a given value of N) will be inversely proportional to η_{coll}. Accordingly, the values at high carrier density could be within the range of $B_{450} = 0.33 - 1.5 \times 10^{-11}$cm^{3}s^{-1}, and $B_{520} = 0.4 - 2 \times 10^{-12}$cm^{3}s^{-1}. The uncertainty in η_{coll} affects the value of C though changing the radiative current, and hence I_c in Eq. 6; the effect of this will depend on the relative importance of the three recombination processes considered here. To understand this, we have analysed the data presented here, but with the upper and lower bounds for the collection efficiency, as discussed above. We find that the change in the value of C is of the order of 15% over the full range of reasonable estimates for collection efficiency; lower than the standard deviation of the values obtained from the individual pixels (about 30%). This low influence in the value of B is to be expected if the current through the device is dominated by non-radiative recombination processes. There is also a ~60% uncertainty in the value of C arising from the value chosen above for η_{inj}. This can be seen to be relatively small, when compared to the large spread of

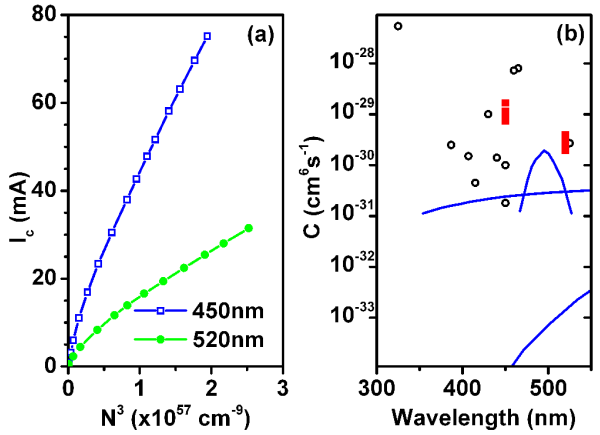

FIG. 4. (a) The Auger current I_c as defined in equation 6, plotted against N^3 for 44μm diameter 450nm emitting and 54μm diameter, 520nm emitting devices. The Auger coefficient C is given by the slope of this graph. (b) Values of the Auger coefficient C found in this work, and reported in the literature. The red squares show the values of C obtained from the work presented here; each symbol represents the value of C obtained from an individual device. Black open symbols denote experimental[6,7,25]determinations of C found in the literature, while the blue lines show reported theoretical[26]values for C.

reported values for C shown in Fig. 4.

In conclusion, we have measured the modulation bandwidth of a number of GaN-based micro-LEDs, emitting at 450 and 520nm wavelength. These results were analysed in a rate equation model, making proper allowance for the carrier density dependence of the radiative coefficient, B, which was determined from LI measurements. By doing this, the carrier lifetimes can be understood by considering Shockley-Read-Hall and Auger recombination as the only significant non-radiative recombination mechanisms, and do not require any carrier overflow mechanisms or variation of the injection efficiency to explain them. Values were found for the Auger coefficient of $C_{450} = 1 \pm 0.3 \times 10^{-29}\mathrm{cm}^6\mathrm{s}^{-1}$ and $C_{520} = 3 \pm 1 \times 10^{-30}\mathrm{cm}^6\mathrm{s}^{-1}$.

This work was supported under the EPSRC HYPIX program. We would like to thank Peter Blood and Peter Smowton of Cardiff University and Ian Watson of Strathclyde University for fruitful discussions.

[1]J. J. D. McKendry, R. P. Green, A. E. Kelly, Z. Gong, B. Guilhabert, D. Massoubre, E. Gu, and M. D. Dawson, IEEE Phot. Tech. Lett. **22**, 1346 (2010).

[2]J. J. D. McKendry, D. Massoubre, S. Zhang, B. R. Rae, R. P. Green, E. Gu, R. K. Henderson, A. E. Kelly, and M. D. Dawson, IEEE J. Lightwave Tech. **30**, 61 (2012).

[3]M. Akhter, P. Maaskant, B. Roycroft, B. Corbett, P. de Mierry, B. Beaumont, and K. Panzer, Electronics Lett. **38**, 1457 (2002) .

[4]B. R. Rae, J. Yang, J. McKendry, Z. Gong, D. Renshaw, J. M. Girkin, E. Gu, M. D. Dawson, and R. K. Henderson, IEEE Trans. Biomed. Circuits and Systems **4**, 437 (2010).

[5]M.-H. Kim, M. F. Schubert, Q. Dai, J. K. Kim, E. F. Schubert, J. Piprek, and Y. Park, Appl. Phys. Lett. **91**, 183507 (2007) .

[6]A. David and M. J. Grundmann, Appl. Phys. Lett. **96**, 103504 (2010) .

[7]W. G. Scheibenzuber, U. T. Schwarz, L. Sulmoni, J. Dorsaz, J.-F. Carlin, and N. Grandjean, J. Appl. Phys. **109**, 093106 (2011).

[8]J. Lee, X. Li, X. Ni, U. Özgür, H. Morkoc, T. Paskova, G. Mulholland, and K. R. Evans, Appl. Phys. Lett. **95**, 201113 (2009).

[9]I. A. Pope, P. M. Smowton, P. Blood, J. D. Thomson, M. J. Kappers, and C. J. Humphreys, Appl. Phys. Lett. **82**, 2755 (2003).

[10]B. Monemar and B. E. Sernelius, Appl. Phys. Lett. **91**, 181103 (2007).

[11]N. I. Bochkareva, V. V. Voronenkov, R. I. Gorbunov, A. S. Zubrilov, Y. S. Lelikov, P. E. Latyshev, Y. T. Rebane, A. I. Tsyuk, and Y. G. Shreter, Appl. Phys. Lett. **96**, 133502 (2010).

[12]G. P. Agrawal, *Long wavelength semiconductor lasers* (Kluwer, 1986) ISBN 0442209959.

[13]F. Stern, J. Appl. Phys. **47**, 5382 (1976).

[14]P. G. Eliseev, H. Li, and I. V. Akimova Appl. Phys. Lett. **75**, 3838 (1999).

[15]E. Schubert, *Light Emitting Diodes*, (Second edition, Cambridge University Press, 2006) ISBN 978-0521865388, p393.

[16]G. H. B. Thompson, Electronics Lett. **19**, 154 (1983).

[17]C. Huh, K.-S. Lee, E.-J. Kang, and S.-J. Park, J. Appl. Phys. **93**, 9383 (2003).

[18]T.-X. Lee, K.-F. Gao, W.-T. Chien, and C.-C. Sun, Optics Express **15**, 6670 (2007).

[19]M.H. Crawford, IEEE J. Sel. Topics. in Quant. Elect. **15**, 1028 (2009).

[20]A. Laubsch, M. Sabathil, J. Baur, M. Peter, and B. Hahn ,IEEE Trans. Elect. Dev. **57**, 79 (2010).

[21]M. Meneghini, N. Trivellin, G. Meneghesso, E. Zanoni, U. Zehnder, and B. Hahn, J. Appl. Phys. **106**, 114508 (2009) .

[22]F. Wang, X. G. Guo, and J. C. Cao, J. Appl. Phys. **108**, 083714 (2010).

[23]Y. J. Lee, J. M. Hwang, T. C. Hsu, M. H. Hsieh, M. J. Jou, B. J. Lee, T. C. Lu, H. C. Kuo and S. C. Wang, IEEE Phot. Tech. Lett. **18**, 1152 (2006).

[24]J.-H. Shin and Y. H. Lee, Appl. Phys. Lett. **67**, 314 (2001).

[25]Y. Shen, G. Mueller, S. Watanabe, N. Gardner, A. Munkholm, and M. Krames, Appl. Phys. Lett. **91**, 141101 (2007); M. Shatalov, A. Chitnis, A. Koudymov, J. Zhang, V. Adivarahan, G. Simin, and M. Khan, Jap. J. Appl. Phys. **41**, L1146 (2002); Q. Dai, Q. Shan, J. Wang, S. Chhajed, J. Cho, E. Schubert, M. Crawford, D. Koleske, M. Kim, and Y. Park, Appl. Phys. Lett. **97**, 133507 (2010); H. Ryu, H. Kim, and J. Shim, *ibid.* **95**, 081114 (2009); M. Zhang, P. Bhattacharya, J. Singh, and J. Hinckley, *ibid.* **95**, 201108 (2009).

[26]K. Delaney, P. Rinke, and C. Van de Walle, Appl. Phys. Lett. **94**, 191109 (2009); E. Kioupakis, P. Rinke, K. Delaney, and C. Van de Walle, *ibid.* **98**, 161107 (2011); F. Bertazzi, M. Goano, and E. Bellotti, *ibid.* **97**, 231118 (2010).